JOC The Journal of Organic Chemistry

Note

pubs.acs.org/joc

Nonstatistical Dynamics in the Thermal Garratt–Braverman/[1,5]-H Shift of One Ene–diallene: An Experimental and Computational Study

Debabrata Samanta, Anup Rana, and Michael Schmittel*

Department of Chemistry and Biology, Universität Siegen, Adolf-Reichwein-Strasse, D-57068 Siegen, Germany

Supporting Information

ABSTRACT: A mechanistic study of the thermal Garratt–Braverman/[1,5]-H shift of ene–diallene **6** leading to alkenes (*E*)-**8** and (*Z*)-**8** is reported. The product ratio was found to be temperature-independent and does not agree with the computed energy barriers (i.e., $\mathbf{TS2_E}^{\ddagger}$ and $\mathbf{TS2_Z}^{\ddagger}$). On the basis of experimental and DFT computational results, we propose a mechanism that is strongly controlled by nonstatistical dynamic effects.

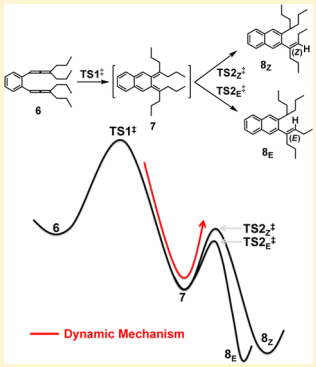

In recent years, a range of reactions has been identified for which transition-state theory (TST) is inadequate to predict the product selectivity because those reaction pathways are intrinsically controlled by *dynamic effects*.[1] Such behavior allows the trajectories to proceed with *continuation of momentum* after crossing the initial TS to show either non-IRC[2] or IRC[3] dynamics in the reaction mechanism. In most cases, an important experimental indicator for the occurrence of such anomalous mechanisms is temperature independence of the product selectivity if the activation enthalpy difference between the selectivity-determining TSs is not zero.[1a,4]

Reactions that involve the formation of a reactive intermediate[5] followed by highly exergonic hydrogen migration or transfer are particularly prone to be influenced by the previous transition state and by nonstatistical dynamics.[6] For instance, hydrogen migration from the thermally activated σ,π-diradical generated in the C^2–C^6 cyclization of enyne–allenes[7] was found to exhibit dynamic effects.[6b,c] To address a more recent example, Carpenter and co-workers have observed that the [1,5]-H shift in an activated cyclopentadiene takes place along a nonstatistical dynamic scenario.[6g] Such findings suggest the need to carefully screen further related reactions. It is well-accepted that the Garratt–Braverman cyclization[8−10] of diallenes[11] (Scheme 1) often involves the generation of a diradical,[12] as inferred by trapping of the corresponding intermediate[13] and by the observation that the rate is independent of the solvent polarity.[8] The thermally generated diradical is well-known to undergo intramolecular follow-up processes, such as formal Diels–Alder,[14] ene,[15] or formal [2 + 2] cycloadditions,[12,16] depending on the nature of substituents.

In 1990, Braverman and Duar[15] showed that conjugated diallenes **1** undergo thermal cyclization to furnish **3** (Scheme 1).

Scheme 1. Garratt–Braverman/[1,5]-H Migration Reaction of Ene–diallenes[15]

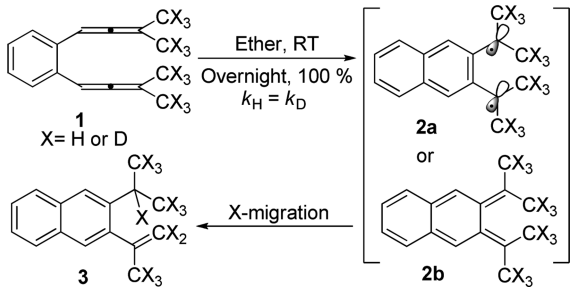

Whether intermediate **2** is a diradical (**2a**) or a bis(*exo*-methylene) compound (**2b**) depends on the steric bulk at the exocyclic double bonds. The observation of an identical reaction rate for both the protio and deuterio analogues of **1** indicated a stepwise pathway in which H or D migration does not take place in the rate-determining step.

To evaluate the possibility of the occurrence of nonstatistical dynamics in the Garratt–Braverman/[1,5]-H shift experimentally, we incorporated *n*-propyl groups at the allene termini (see compound **6**) to open the possibility of (*E*) and (*Z*)-alkene formation (see Scheme 3). The finding of a temperature-independent $\mathbf{8_E}$:$\mathbf{8_Z}$ product ratio, contradicting DFT computational results, led us to conclude that the hydrogen migration takes place under nonstatistical dynamic conditions.

Received: June 13, 2014
Published: August 15, 2014

   dx.doi.org/10.1021/jo501324w | J. Org. Chem. 2014, 79, 8435–8439

Ene−diallene **6** was synthesized in two steps as depicted in Scheme 2. The formation of the allene subunit was confirmed

Scheme 2. Synthesis of Ene−diallene 6

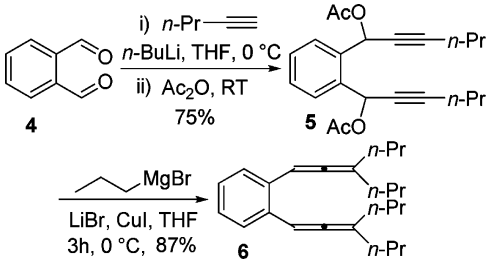

by following the disappearance of the ^{1}H NMR signal at 2.1 ppm ($C\underline{H}_3CO-$ of **5**) and the appearance of the highly characteristic allene carbon ($C=\underline{C}=C$) signal located at 203.1 ppm in the ^{13}C NMR spectrum.

To examine the effect of temperature on the product selectivity, the thermolysis of **6** was performed in dry and degassed toluene at different temperatures controlled to ±0.1 °C (Scheme 3). The geometrical isomers $\mathbf{8_E}$ and $\mathbf{8_Z}$ produced upon

Scheme 3. Thermolysis of Ene−diallene 6 Producing $\mathbf{8_Z}$ and $\mathbf{8_E}$

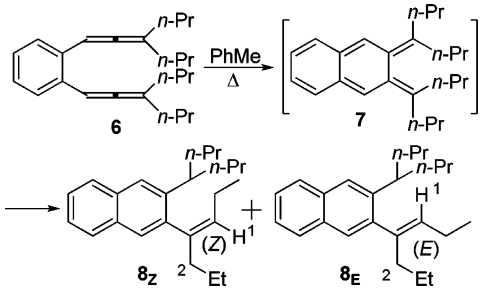

thermolysis were separated by long-bed flash column chromatography, characterized as pure compounds by elemental analysis, and structurally identified by ^{1}H, ^{13}C, ^{1}H,^{1}H COSY, and ^{1}H,^{1}H NOESY NMR techniques. The presence of a characteristic correlation signal between protons 1-H and 2-H in the ^{1}H,^{1}H NOESY spectrum served to identify isomer $\mathbf{8_Z}$, while in $\mathbf{8_E}$ no correlation signal was detected.

In the thermolysis of **6** in toluene, the experimental $\mathbf{8_E}$:$\mathbf{8_Z}$ product ratio was constant at 10.3:1 over the whole temperature range of 60−140 °C (Table 1). In CCl_4 (i.e., a solvent with a sparse vibrational manifold), the $\mathbf{8_E}$:$\mathbf{8_Z}$ product ratio was equally constant at 10.0:1.[17] Such a finding is strongly indicative of the occurrence of nonstatistical dynamics in the reaction mechanism. Moreover, the DFT-predicted $\mathbf{8_E}$:$\mathbf{8_Z}$ ratios[18] (Figure 1) were neither in quantitative agreement with the experimental ratios nor reflective of temperature independence.

We utilized the (BS)-UB3LYP hybrid density functional in conjunction with the 6-31G(d,p) basis set because the predicted activation enthalpy of the [1,5]-H shift in *s-trans-cis*-1,3-pentadiene using the B3LYP/6-31G(d) method[19] is 36.6 kcal mol^{-1}, which is very close to the best value (38.4 kcal mol^{-1}) obtained by Lynch and Truhlar.[20] Solvent effects were recognized by implementing the polarizable continuum model (PCM). Free energy values are reported at 25 °C referenced to the most stable conformer **6**. Moreover, the thermochemical analysis of $\mathbf{TS2_E}^{\ddagger}$ and $\mathbf{TS2_Z}^{\ddagger}$ was performed at various temperatures.

Table 1. Experimental and Calculated $\mathbf{8_Z}$:$\mathbf{8_E}$ Product Ratios in the Thermolysis of Ene−diallene 6 in Toluene

temp (°C)	time (min)	exptl $\mathbf{8_E}$:$\mathbf{8_Z}$ ratio[a]	$\Delta\Delta G^{\ddagger}$[b]	calcd $\mathbf{8_E}$:$\mathbf{8_Z}$ ratio[c]
60	60	10.3:1	2.35	34.9:1
80	40	10.4:1	2.41	31.1:1
100	20	10.4:1	2.46	27.7:1
120	10	10.3:1	2.51	24.9:1
140	7	10.3:1	2.56	22.7:1

[a]Ratios were determined from the ^{1}H NMR signals of the crude reaction mixture after thermolysis at a standard deviation of ±0.05. [b]Free energy differences (in kcal mol^{-1}), $\Delta\Delta G^{\ddagger} = \Delta G^{\ddagger}_{TS2_Z} - \Delta G^{\ddagger}_{TS2_E}$, at different temperatures were obtained from DFT computations (see the text). [c]Ratios were calculated from the computed $\Delta\Delta G^{\ddagger}$ values using TST.

The overall reactions toward $\mathbf{8_Z}$ and $\mathbf{8_E}$ were found to be highly exothermic, with ΔG = −46.09 and −50.47 kcal mol^{-1}, respectively. Because of the strong steric congestion about the *n*-propyl chains, the reactive conformer of ene−diallene **6a** is destabilized by 12.31 kcal mol^{-1} versus the most stable conformer **6**. The intermediate **INT** generated after C−C bond formation is a completely conjugated system, which is more stable than ene−diallene **6** by 14.60 kcal mol^{-1}. The NBO analysis of **INT** using the B3LYP/cc-PVTZ method showed the absence of any unpaired electron. Moreover, the analysis based on second-order perturbation theory suggested a strong resonance interaction of each exocyclic double bond in **INT** with the nearest endocyclic double bond (7.27 kcal mol^{-1}) and a weak interaction with the other exocyclic double bond (4.05 kcal mol^{-1}). Since the initial transition state $\mathbf{TS1}^{\ddagger}$ involving the C−C bond formation is located at 30.92 kcal mol^{-1}, the formation of **INT** releases 45.52 kcal mol^{-1} potential energy that is transformed into kinetic energy during the process. From intermediate **INT**, two reaction paths evolve to the hydrogen migration products $\mathbf{8_Z}$ and $\mathbf{8_E}$ via $\mathbf{TS2_Z}^{\ddagger}$ ($\Delta G^{\ddagger}$ = 2.75 kcal mol^{-1}) and $\mathbf{TS2_E}^{\ddagger}$ ($\Delta G^{\ddagger}$ = 0.49 kcal mol^{-1}), respectively. Remarkably, the two follow-up TSs $\mathbf{TS2_Z}^{\ddagger}$ and $\mathbf{TS2_E}^{\ddagger}$ are excessively lower in energy compared with the initial transition state $\mathbf{TS1}^{\ddagger}$ by 28.17 and 30.43 kcal mol^{-1}, respectively. Therefore, after crossing the initial transition state $\mathbf{TS1}^{\ddagger}$, the reacting molecules acquire a large excess of kinetic energy on the way to intermediate **INT** and therefore easily overcome the follow-up barrier, $\mathbf{TS2_E}^{\ddagger}$ or $\mathbf{TS2_Z}^{\ddagger}$, in a direct conservation of momentum before losing the kinetic energy from the reacting vibrational mode to other modes or to the bath. It might look unusual to observe such a mechanism on crossing such a deep intermediate well, but the occurrence of dynamics on such deep wells is known in the literature.[6a,g,21] Indeed, a few initial trajectory computations on **1** (X = H) performed at the UBLYP/3-21G level showed hydrogen migration to occur within <50 fs after $\mathbf{TS1}^{\ddagger}$.[22] Moreover, further mechanistic options such as tunneling or crossing between singlet and triplet are easily discarded by distance[23] and energy[24] arguments.

We also investigated how the preferential formation of $\mathbf{8_E}$ over $\mathbf{8_Z}$ can be understood on the basis of dynamics. Structurally, an increase in the C1−C2−C3−C4 dihedral angle (Figure 2) from intermediate **INT** is necessary to reach $\mathbf{TS2_E}^{\ddagger}$ (110.8° → 165.7°), whereas a decrease leads toward $\mathbf{TS2_Z}^{\ddagger}$ (110.8° → 70.2°). On the way from $\mathbf{TS1}^{\ddagger}$ to **INT**, the dihedral angle widens from 64.1° to 110.8°, and therefore, under dynamic conditions a supportive momentum toward $\mathbf{TS2_E}^{\ddagger}$ is generated, preferably yielding $\mathbf{8_E}$ in an excess amount.

dx.doi.org/10.1021/jo501324w | J. Org. Chem. 2014, 79, 8435−8439

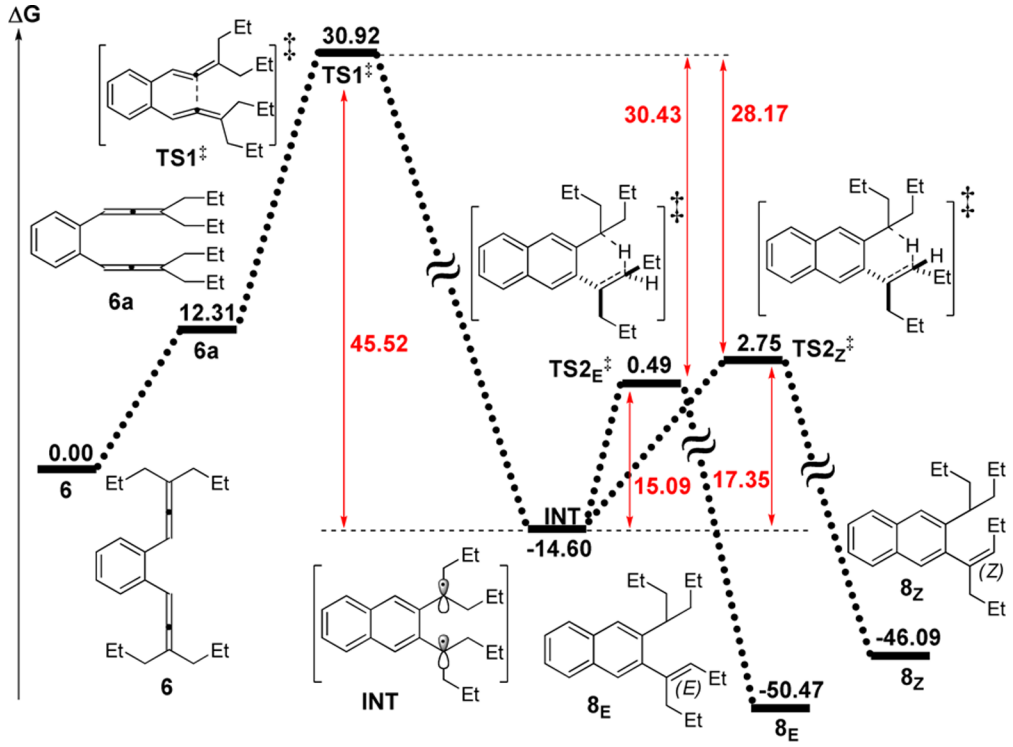

Figure 1. Reaction profile for the thermal cyclization of **6** in toluene (PCM) at the (BS)-UB3LYP/6-31G(d,p) level. Relative free energies at 25 °C are given in kcal mol^{-1}. The crucial energy differences are highlighted in red.

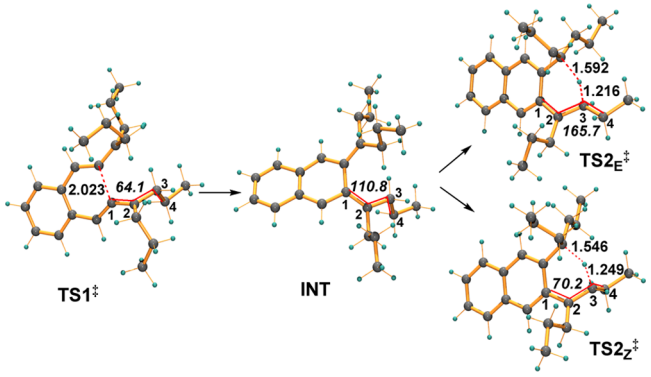

Figure 2. Optimized structures of TSs **TS1**‡, **TS2**$_E$‡, and **TS2**$_Z$‡ and intermediate **INT**, with distances (in Å) shown in roman type and dihedral angles (in deg) shown in italics.

Coincidentally, in this case the dynamic preference for **8**$_E$ over **8**$_Z$ is in agreement with that suggested by TST.

In summary, we have presented a system in which the selectivity after [1,5]-H migration leading to products **8**$_E$ and **8**$_Z$ is temperature-independent over a temperature range of 80 °C and does not agree with the free energy differences and the temperature dependence as derived from the computed TSs **TS2**$_E$‡ and **TS2**$_Z$‡. These two findings and hydrogen migration within 50 fs strongly suggest that the reacting molecules comply with nonstatistical dynamics during product formation.

EXPERIMENTAL SECTION

General Procedures and Characterization. All reagents were purchased commercially and utilized without further purification. The solvents were dried with proper desiccants and distilled prior to use. Silica gel (0.035−0.070 mm) was used for column chromatography. The following abbreviations are used to describe NMR peak patterns: s = singlet, t = triplet, dd = doublet of doublets, dq = doublet of quartets, m = multiplet. The numbering of carbon atoms in the molecular formulas is used only for assignment of NMR signals and thus is not necessarily in accordance with IUPAC nomenclature rules. 1,1′-(1,2-Phenylene)-bis(hex-2-yne-1,1-diyl) diacetate (**5**) was prepared according to the reported procedure.[25]

Computations. We utilized the (BS)-UB3LYP hybrid density functional in conjunction with the 6-31G(d,p) basis set, applying tight convergence criteria and the ultrafine grid integral algorithm to optimize stationary points and TS structures. All of the computed minima and first-order saddle point structures were verified by examining the harmonic vibrational frequencies via their analytical second derivatives because they should have zero and one imaginary frequency, respectively. Furthermore, intrinsic reaction coordinate (IRC) computations were carried out to verify the optimized TSs.

1,2-Bis(3-propylhexa-1,2-dienyl)benzene (6).

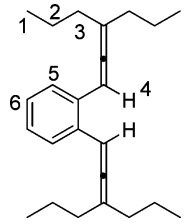

A solution of *n*-propylmagnesium bromide (54.3 mmol) [prepared from *n*-propyl bromide (4.93 mL, 54.3 mmol) and magnesium (1.30 g, 54.3 mmol) in 100 mL of dry THF] was added dropwise to a well-stirred mixture of LiBr (9.43 g, 108 mmol) and CuI (10.3 g, 54.3 mmol) in 100 mL of dry THF at 0 °C under a nitrogen atmosphere. After the resultant solution was stirred for 15 min at the same temperature, propargyl acetate **5** (2.50 g, 6.78 mmol) in 30 mL of dry THF was added. Stirring was continued for another 3 h at 0 °C to complete the reaction. Then the reaction was quenched with saturated ammonium chloride solution. The aqueous layer was extracted with diethyl ether (3 × 25 mL). The combined organic layers were dried over $MgSO_4$ and concentrated using a rotary evaporator. After purification by flash column chromatography, (silica gel, *n*-pentane, R_f = 0.68),

dx.doi.org/10.1021/jo501324w | J. Org. Chem. 2014, 79, 8435−8439

ene−diallene **6** (1.90 g, 87%) was isolated as a colorless oil. IR (KBr): $\tilde{\nu}$ 3060, 2959, 2873, 1945, 1599, 1458, 1377, 1336, 1281, 1181, 1335, 1072, 1037, 957, 807, 751 cm^{-1}. ^1H NMR (400 MHz, $C_2D_2Cl_4$): δ = 0.90 (t, ^3J = 7.4 Hz, 12H, 1-H), 1.47 (sextet, ^3J = 7.4 Hz, 8H, 2-H), 1.94−2.08 (m, 8H, 3-H), 6.44 (quintet, ^5J = 2.8 Hz, 2H, 4-H), 7.07 (dd, ^3J = 5.8 Hz, ^4J = 3.4 Hz, 2H, 6-H), 7.32 (dd, ^3J = 5.8 Hz, ^4J = 3.4 Hz, 2H, 5-H) ppm. ^{13}C NMR (100 MHz, $C_2D_2Cl_4$): δ = 14.0, 20.9, 34.7, 91.8, 107.5, 126.2, 127.5, 132.4, 203.1 ppm. Anal. Calcd for $C_{24}H_{34}$: C, 89.37; H, 10.63. Found: C, 89.33; H, 10.92.

Thermolysis of 1,2-Bis(3-propylhexa-1,2-dienyl)benzene (6). A solution of ene−diallene **6** (500 mg, 1.55 mmol) in dry and degassed toluene (25 mL) was placed in a sealed tube and heated for 1 h at 140 °C to complete the cyclization. After removal of toluene under reduced pressure and purification by flash column chromatography (silica gel, *n*-pentane, R_{f1} = 0.61 and R_{f2} = 0.57), (*E*)-2-(hept-3-en-4-yl)-3-(heptan-4-yl)naphthalene ($\mathbf{8_E}$) and (*Z*)-2-(hept-3-en-4-yl)-3-(heptan-4-yl)naphthalene ($\mathbf{8_Z}$) were isolated.

*(E)-2-(Hept-3-en-4-yl)-3-(heptan-4-yl)naphthalene (**8$_E$**).*

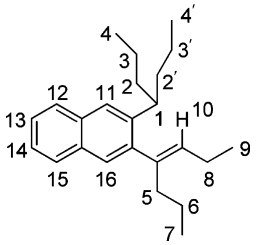

R_f = 0.61 (*n*-pentane); colorless oil. Isolated yield: 73% (365 mg, 1.13 mmol). IR (KBr): $\tilde{\nu}$ 3053, 2957, 2868, 1591, 1458, 1376, 1271, 1211, 1103, 949, 883, 745 cm^{-1}. ^1H NMR (400 MHz, $C_2D_2Cl_4$): δ = 0.77 (t, ^3J = 7.4 Hz, 6H, 4-H, 4′-H), 0.81 (t, ^3J = 7.2 Hz, 3H, 7-H), 0.98 (t, ^3J = 7.4 Hz, 3H, 9-H), 1.04−1.31 (m, 6H, 3-H, 3′-H, 6-H), 1.44−1.62 (m, 4H, 2-H, 2′-H), 2.14 (quintet, ^3J = 7.4 Hz, 2H, 8-H), 2.20−2.30 (m, 2H, 5-H), 2.78 (quintet, ^3J = 7.1 Hz, 1H, 1-H), 5.23 (t, ^3J = 7.4 Hz, 1H, 10-H), 7.29−7.35 (m, 2H, 13-H, 14-H), 7.38 (s, 1H, 11-H), 7.53 (s, 1H, 16-H), 7.66−7.71 (m, 2H, 12-H, 15-H) ppm. ^{13}C NMR (100 MHz, $C_2D_2Cl_4$): δ = 14.2, 14.5 (2C), 20.8, 21.4 (2C), 34.5, 39.6, 39.9, 124.0, 124.8, 125.0, 127.2, 127.3, 127.4, 131.1, 132.4, 132.4, 139.8, 144.0, 144.0 ppm. Anal. Calcd for $C_{24}H_{34}$: C, 89.37; H, 10.63. Found: C, 89.30; H, 10.82.

*(Z)-2-(Hept-3-en-4-yl)-3-(heptan-4-yl)naphthalene (**8$_Z$**).* R_f = 0.57 (*n*-pentane); colorless oil. Isolated yield: 8% (40.0 mg, 124 μmol). IR (KBr): $\tilde{\nu}$ 3053, 2956, 2868, 1493, 1457, 1375, 1268, 1138, 1099, 1015, 948, 888, 744 cm^{-1}. ^1H NMR (400 MHz, $C_2D_2Cl_4$): δ = 0.73 (t, ^3J = 7.4 Hz, 3H, 4-H or 4′-H), 0.79−0.85 (m, 9H, 4′-H or 4-H, 7-H, 9-H),

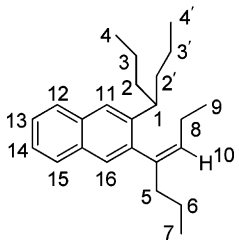

0.97−1.79 (m, 12H, 2-H, 2′-H, 3-H, 3′-H, 6-H, 8-H), 2.14 (t, ^3J = 7.6 Hz, 2H, 5-H), 2.73 (quintet, ^3J = 6.89 Hz, 1H, 1-H), 5.45 (t, ^3J = 7.2 Hz, 1H, 10-H), 7.30−7.36 (m, 3H, 11-H, 13-H, 14-H), 7.58 (s, 1H, 16-H), 7.67−7.73 (m, 2H, 12-H, 15-H) ppm. ^{13}C NMR (100 MHz, $C_2D_2Cl_4$): δ = 13.9, 14.4, 14.4, 14.6, 20.6, 21.0, 21.2, 22.8, 38.8, 39.6, 40.2, 41.0, 124.3, 124.8, 125.0, 127.3, 127.4, 127.6, 129.9, 131.2, 132.4, 139.7, 140.4, 144.0 ppm. Anal. Calcd for $C_{24}H_{34}$: C, 89.37; H, 10.63. Found: C, 89.08; H, 10.78.

■ ASSOCIATED CONTENT

Ⓢ Supporting Information

Spectroscopic and computational data. This material is available free of charge via the Internet at http://pubs.acs.org.

■ AUTHOR INFORMATION

Corresponding Author

*E-mail: schmittel@chemie.uni-siegen.de.

Notes

The authors declare no competing financial interest.

■ ACKNOWLEDGMENTS

We are indebted to the Deutsche Forschungsgemeinschaft for financial support (Schm 647/18-1) and to Prof. Ralph Jaquet (Universität Siegen) for helpful support concerning the computational infrastructure. This work is dedicated to Prof. Dr. Ch. Rüchardt on the occasion of his 85th birthday.

■ REFERENCES

(1) (a) Carpenter, B. K. *Acc. Chem. Res.* **1992**, *25*, 520. (b) Carpenter, B. K. *Angew. Chem.* **1998**, *110*, 3532. (c) Carpenter, B. K. *Chem. Soc. Rev.* **2006**, *35*, 736. (d) Oyola, Y.; Singleton, D. A. *J. Am. Chem. Soc.* **2009**, *131*, 3130. (e) Zheng, J.; Papajak, E.; Truhlar, D. G. *J. Am. Chem. Soc.* **2009**, *131*, 15754. (f) Glowacki, D. R.; Liang, C. H.; Marsden, S. P.; Harvey, J. N.; Pilling, M. J. *J. Am. Chem. Soc.* **2010**, *132*, 13621. (g) Quijano, L. M. M.; Singleton, D. A. *J. Am. Chem. Soc.* **2011**, *133*, 13824. (h) Lan, Y.; Danheiser, R. L.; Houk, K. N. *J. Org. Chem.* **2012**, *77*, 1533. (i) Carpenter, B. K. *Chem. Rev.* **2013**, *113*, 7265. (j) Biswas, B.; Collins, S. C.; Singleton, D. A. *J. Am. Chem. Soc.* **2014**, *136*, 3740. (k) Samanta, D.; Rana, A.; Schmittel, M. *J. Org. Chem.* **2014**, *79*, 2368.

(2) (a) Sun, L.; Song, K.; Hase, W. L. *Science* **2002**, *296*, 875. (b) Debbert, S. L.; Carpenter, B. K.; Hrovat, D. A.; Borden, W. T. *J. Am. Chem. Soc.* **2002**, *124*, 7896. (c) Ammal, S. C.; Yamataka, H.; Aida, M.; Dupuis, M. *Science* **2003**, *299*, 1555. (d) Ussing, B. R.; Hang, C.; Singleton, D. A. *J. Am. Chem. Soc.* **2006**, *128*, 7594. (e) Wang, Z.; Hirschi, J. S.; Singleton, D. A. *Angew. Chem., Int. Ed.* **2009**, *48*, 9156. (f) Andujar-De Sanctis, I. L.; Singleton, D. A. *Org. Lett.* **2012**, *14*, 5238.

(3) (a) Houston, P. L.; Kable, S. H. *Proc. Natl. Acad. Sci. U.S.A.* **2006**, *103*, 16079. (b) Glowacki, D. R.; Marsden, S. P.; Pilling, M. J. *J. Am. Chem. Soc.* **2009**, *131*, 13896. (c) Jordan, M. J. T.; Kable, S. H. *Science* **2012**, *335*, 1054.

(4) (a) Carpenter, B. K. *J. Am. Chem. Soc.* **1985**, *107*, 5730. (b) Samanta, D.; Cinar, M. E.; Das, K.; Schmittel, M. *J. Org. Chem.* **2013**, *78*, 1451.

(5) (a) Abe, M. *Chem. Rev.* **2013**, *113*, 7011. (b) Mohamed, R. K.; Peterson, P. W.; Alabugin, I. V. *Chem. Rev.* **2013**, *113*, 7089. (c) Peterson, P. W.; Mohamed, R. K.; Alabugin, I. V. *Eur. J. Org. Chem.* **2013**, 2505.

(6) (a) Osterheld, T. H.; Brauman, J. I. *J. Am. Chem. Soc.* **1993**, *115*, 10311. (b) Bekele, T.; Christian, C. F.; Lipton, M. A.; Singleton, D. A. *J. Am. Chem. Soc.* **2005**, *127*, 9216. (c) Schmittel, M.; Vavilala, C.; Jaquet, R. *Angew. Chem., Int. Ed.* **2007**, *46*, 6911. (d) Zhou, J.; Schlegel, H. B. *J. Phys. Chem. A* **2009**, *113*, 1453. (e) Zhou, J.; Schlegel, H. B. *J. Phys. Chem. A* **2009**, *113*, 9958. (f) Hong, Y. J.; Tantillo, D. J. *Nat. Chem.* **2009**, *1*, 384. (g) Goldman, L. M.; Glowacki, D. R.; Carpenter, B. K. *J. Am. Chem. Soc.* **2011**, *133*, 5312. (h) Hong, Y. J.; Tantillo, D. J. *Nat. Chem.* **2014**, *6*, 104.

(7) (a) Schmittel, M.; Strittmatter, M.; Kiau, S. *Tetrahedron Lett.* **1995**, *36*, 4975. (b) Schmittel, M.; Kiau, S.; Siebert, T.; Strittmatter, M. *Tetrahedron Lett.* **1996**, *37*, 7691. (c) Schmittel, M.; Maywald, M.; Strittmatter, M. *Synlett* **1997**, 165. (d) Schmittel, M.; Vavilala, C.; Cinar, M. E. *J. Phys. Org. Chem.* **2012**, *25*, 182.

(8) Braverman, S.; Segev, D. *J. Am. Chem. Soc.* **1974**, *96*, 1245.

(9) Garratt, P. J.; Neoh, S. B. *J. Am. Chem. Soc.* **1975**, *97*, 3255.

(10) (a) Basak, A.; Das, S.; Mallick, D.; Jemmis, E. D. *J. Am. Chem. Soc.* **2009**, *131*, 15695. (b) Maji, M.; Mallick, D.; Mondal, S.; Anoop, A.; Bag, S. S.; Basak, A.; Jemmis, E. D. *Org. Lett.* **2011**, *13*, 888. (c) Mondal, S.; Mitra, T.; Mukherjee, R.; Addy, P. S.; Basak, A. *Synlett* **2012**, *23*, 2582.

(11) Hopf, H.; Markopoulos, G. *Beilstein J. Org. Chem.* **2012**, *8*, 1936.

(12) Skraba, S. L.; Johnson, R. P. *J. Org. Chem.* **2012**, *77*, 11096.

(13) (a) Cheng, Y. S. P.; Garratt, P. J.; Neoh, S. B.; Rumjanek, V. M. *Isr. J. Chem.* **1985**, *26*, 101. (b) Greenberg, M. M.; Blackstock, S. C.; Berson, J. A. *Tetrahedron Lett.* **1987**, *28*, 4263.
(14) (a) Rodríguez, D.; Castedo, L.; Domínguez, D.; Saá, C. *Org. Lett.* **2003**, *5*, 3119. (b) Kitagaki, S.; Ohdachi, K.; Katoh, K.; Mukai, C. *Org. Lett.* **2006**, *8*, 95. (c) Lin, Y.-C.; Lin, C.-H. *Org. Lett.* **2007**, *9*, 2075. (d) Addy, P. S.; Dutta, S.; Biradha, K.; Basak, A. *Tetrahedron Lett.* **2012**, *53*, 19.
(15) Braverman, S.; Duar, Y. *J. Am. Chem. Soc.* **1990**, *112*, 5830.
(16) (a) Jacobs, T. L.; McClenon, J. R.; Muscio, O. J., Jr. *J. Am. Chem. Soc.* **1969**, *91*, 6038. (b) Johnson, R. P. *Chem. Rev.* **1989**, *89*, 1111. (c) Alcaide, B.; Almendros, P.; Aragoncillo, C. *Chem. Soc. Rev.* **2010**, *39*, 783.
(17) The thermolysis of **6** in CCl_4 at 60, 80, and 100 °C generated a constant $\mathbf{8}_E$:$\mathbf{8}_Z$ product ratio of (10.00 ± 0.05):1. Hence, the use of CCl_4 as solvent led to a very minor increase in dynamic contributions compared with toluene.
(18) Frisch, M. J.; Trucks, G. W.; Schlegel, H. B.; Scuseria, G. E.; Robb, M. A.; Cheeseman, J. R.; Scalmani, G.; Barone, V.; Mennucci, B.; Petersson, G. A.; Nakatsuji, H.; Caricato, M.; Li, X.; Hratchian, H. P.; Izmaylov, A. F.; Bloino, J.; Zheng, G.; Sonnenberg, J. L.; Hada, M.; Ehara, M.; Toyota, K.; Fukuda, R.; Hasegawa, J.; Ishida, M.; Nakajima, T.; Honda, Y.; Kitao, O.; Nakai, H.; Vreven, T.; Montgomery, J. A., Jr.; Peralta, J. E.; Ogliaro, F.; Bearpark, M.; Heyd, J. J.; Brothers, E.; Kudin, K. N.; Staroverov, V. N.; Kobayashi, R.; Normand, J.; Raghavachari, K.; Rendell, A.; Burant, J. C.; Iyengar, S. S.; Tomasi, J.; Cossi, M.; Rega, N.; Millam, J. M.; Klene, M.; Knox, J. E.; Cross, J. B.; Bakken, V.; Adamo, C.; Jaramillo, J.; Gomperts, R.; Stratmann, R. E.; Yazyev, O.; Austin, A. J.; Cammi, R.; Pomelli, C.; Ochterski, J. W.; Martin, R. L.; Morokuma, K.; Zakrzewski, V. G.; Voth, G. A.; Salvador, P.; Dannenberg, J. J.; Dapprich, S.; Daniels, A. D.; Farkas, Ö.; Foresman, J. B.; Ortiz, J. V.; Cioslowski, J.; Fox, D. J. *Gaussian 09*, revision A.1; Gaussian, Inc.: Wallingford, CT, 2009.
(19) Schmittel, M.; Mahajan, A. A.; Bucher, G.; Bats, J. W. *J. Org. Chem.* **2007**, *72*, 2166.
(20) Lynch, B. J.; Truhlar, D. G. *J. Phys. Chem. A* **2001**, *105*, 2936.
(21) (a) Hrovat, D. A.; Duncan, J. A.; Borden, W. T. *J. Am. Chem. Soc.* **1999**, *121*, 169. (b) Nummela, J. A.; Carpenter, B. K. *J. Am. Chem. Soc.* **2002**, *124*, 8512.
(22) Born−Oppenheimer molecular dynamics trajectory computations on **1** (X = H) were performed at the UBLYP/3-21G level starting from the initial transition state ($\mathbf{TS1}^{\ddagger}$) with a step size of 1 fs. In all trajectories, we observed hydrogen migration within 42−48 fs.
(23) In the present system, the migrating hydrogen has to move by more than 1.4 Å from intermediate **7** to the products. Therefore, the occurrence of tunneling is extremely unlikely.
(24) The triplet manifold lies significantly higher than the singlet manifold (see p 8 in the Supporting Information), precluding product formation from the triplet state.
(25) Inanaga, J.; Sugimoto, Y.; Hanamoto, T. *Tetrahedron Lett.* **1992**, *33*, 7035.